Chapter 6

Gas Phase Synthesis of Charged Copper and Silver Fischer Carbenes from Diazomalonates: Mechanistic and Conformational Considerations in Metal Mediated Wolff Rearrangements

Published previously in: Julian, R. R.; May, J. A.; Stoltz, B. M.; Beauchamp, J. L. *J. Am. Chem. Soc.* **2003**, *125(15)*, 4478-4486.

6.1 Introduction

The gas phase synthesis of metallo-carbenoid compounds has a surprisingly long history.[1] In early studies, the metallo-carbenoids were created by high energy methods utilizing electron impact ionization. The resulting ions were then used in bimolecular reactions with various neutral molecules to study the chemistry of and determine metal-carbon bond strengths for these charged Fischer carbenes. The importance of studying gas phase species in determining the mechanistic pathways for olefin metathesis was also realized early on,[1b] and more recent studies have taken advantage of electrospray ionization (ESI) to continue this work.[2] Gas phase experiments have also enabled mechanistic studies with other highly reactive metallo-carbenoid species.[3]

The utility of diazo compounds as carbene and metallo-carbenoid precursors has been heavily exploited in solution phase chemistry.[4] The use of diazo compounds as precursors in gas phase mass spectrometry (MS) remains less explored. We have recently reported that diazo compounds are excellent carbene precursors for MS.[5] In these experiments, a carbene is produced through the low-energy collision activated dissociation (CAD)[6] of a diazo compound. The resulting loss of N_2 and generation of the carbene is achieved under conditions sufficiently mild that non-covalently bound complexes are not dissociated in the process. The highly reactive carbene then inserts into the guest and converts the noncovalent complex into a covalently bound molecule. All of the molecules in this previous study were based on the diazomalonate core (with at least one 18-crown-6 crown ether attached). These reagents have been appropriately named "molecular mousetraps."[5]

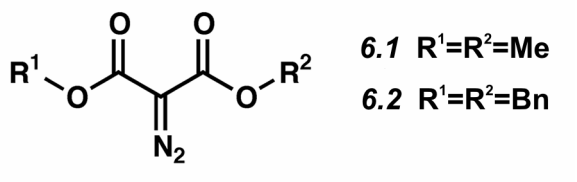

6.1 **$R^1=R^2=Me$**

6.2 **$R^1=R^2=Bn$**

Diazomalonates[7] (such as **6.1** and **6.2** above) and related diazo ketones[8] are known to undergo Wolff rearrangement in the gas phase as shown in Scheme 6.1. Since its discovery in 1902, the Wolff rearrangement[9] has been the subject of numerous studies.[10] In the present work we use the benefits of gas phase experiments to study the mechanism of multiple, consecutive Wolff rearrangements observed in diazomalonates.[7] The effects that various coordinated metal ions and other charged groups have on Wolff rearrangements are discerned from gas phase MS experiments. Theory is used to quantitatively assess each intermediate for the proposed mechanism. Although the solution phase synthesis of stable copper (I) and silver (I) Fischer carbenes has been

known for some time,[11] here we report the first gas phase synthesis of copper (I) and silver (I) Fischer carbenes. The results for several intermolecular reactions of these carbenes with various adduct molecules are presented.

Scheme 6.1

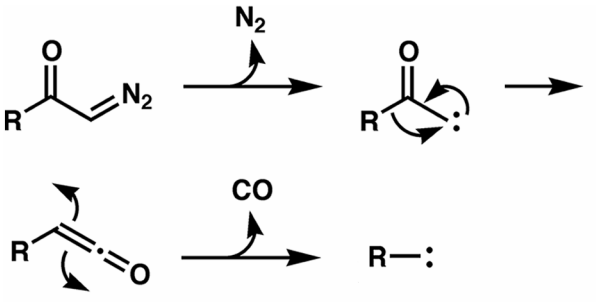

7.2 Experimental Methodology

All mass spectra were acquired on an LCQ Classic instrument from Finnigan. Solutions of the reagents in the ~30-80 μM range were electrosprayed from a ~80/20 (v/v) solution of methanol/water with a minimum of 0.1% MeCN added. Soft ionization settings were used to maximize the intensity of non-covalently bound complexes.[12] Ions of interest were isolated and subjected to collisional activation until product peaks were observed. For each MS^n step, the peak of interest was re-isolated prior to further dissociation. All chemicals were purchased from Sigma-Aldrich and used without further purification unless otherwise noted. Metal ion complexes were formed by adding an appropriate salt to the solution. No counter-ion effects were noted. For studies of intermolecular reactions, the desired ligand (such as 5-hexynenitrile) was added directly to the solution in several-fold excess.

Calculations. Candidate structures were evaluated initially at the PM3 semi-empirical level. Following minimization at the lower level of theory, structures were optimized

using density functional theory (DFT). The DFT calculations were carried out using Jaguar 4.1 (Schrödinger, Inc., Portland, Oregon). Full geometry optimization was performed at the B3LYP/LACVP** level of theory. Semi-empirical PM3 MNDO type calculations were carried out using the HyperChem 5.1 Professional Suite (Hypercube, Inc., Gainesville, Florida).

Synthesis. Reactions were performed in flame-dried glassware under a nitrogen atmosphere. Solvents were dried and purified using activated alumina columns. All other reagents were used as received from commercial sources. Reaction temperatures were controlled by an IKAmag temperature modulator. Thin-layer chromatography (TLC) was performed using E. Merck silica gel 60 F254 precoated plates (0.25 mm) and visualized by UV and *p*-anisaldehyde staining. ICN Silica gel (particle size 0.032-0.063 mm) was used for flash chromatography. ^{1}H NMR spectra were recorded on a Varian Mercury 300 spectrometer (at 300 MHz) in $CDCl_3$ and are internally referenced to the residual chloroform peak (7.27 ppm) relative to Me_4Si. Data for ^{1}H NMR spectra are reported as follows: chemical shift (δ ppm), multiplicity, coupling constant (Hz), and integration. IR spectra were recorded on a Perkin Elmer Paragon 1000 spectrometer and are reported in frequency of absorption (cm^{-1}). Preparatory reversed phase HPLC was performed on a Beckman HPLC with a Waters DeltaPak 25 x 100 mm, 100 μm C18 column equipped with a guard.

2-Diazodimethylmalonate (6.1). **6.1** was prepared according to previously established methods.[13] The product was isolated as a yellow oil (2.58 g, 16.29 mmol, 93% yield) with the same physical properties as previously reported.

2-Diazodibenzylmalonate (6.2). A round-bottomed flask (10 mL) was charged with dibenzylmalonate (77 μL, 0.308 mmol), MeCN (3 mL), and *p*-acetamidobenzylsulfonyl

azide (116 mg, 0.485 mmol). TEA (150 μL, 1.08 mmol) was then added, and the reaction was stirred at room temperature for 10 h. TLC analysis (3:1 hexanes:EtOAc eluent, R_F=0.46) showed the reaction to be complete. The solvent was removed by evaporation under reduced pressure, and the crude mixture was subjected to flash chromatographic purification (5:1 hexanes:EtOAc eluent) to afford **6.2** as a yellow oil (75 mg, 0.242 mmol, 78% yield) with the same physical properties as previously reported. [14]

Diazomalonate 6.25. A round-bottomed flask (5 mL) was charged with CH_2Cl_2 (1 mL), CD_3OD (500 μL, 11.3 mmol), and TEA (100 μL, 0.717 mmol). This mixture was stirred rapidly while malonyldichloride (20 μL, 0.206 mmol) was added dropwise at room temperature. TLC analysis (3:1 hexanes:EtOAc eluent, R_F=0.45) showed complete conversion to the malonate ester within 2 h. The solvent and excess reagents were removed by evaporation under reduced pressure, and then MeCN (2 ml) and *p*-acetamidobenzylsulfonyl azide (103.5 mg, 0.431 mmol) were added to the flask. TEA (100 μL, 0.717 mmol) was added, and the solution was stirred for 24 h. The solvent was then removed by evaporation under reduced pressure. The product was purified by dissolving the residue in a minimal amount of CH_2Cl_2 (500 μL) and then precipitating the salts by addition of Et_2O (5 mL). Filtration through celite removed the salts, and the solvent was removed by evaporation under reduced pressure to afford **6.25** as a yellow oil (11.9 mg, 0.073 mmol, 35% yield).

Diazomalonate 6.26. To a stirred solution of $H_2C(^{13}CO_2H)_2$ (19.7 mg, 0.179 mmol) in Et_2O (2 mL) in a scratch-free flask (25 mL) was added ethereal diazomethane solution (0.2 M, 4.0 mL, 0.800 mmol). TLC analysis (3:1 hexanes:EtOAc eluent, R_F=0.45) showed the reaction to be complete. The solvent and excess reagents were removed by

evaporation under reduced pressure, and then MeCN (1 mL) and *p*-acetamidobenzylsulfonyl azide (25.9 mg, 0.108 mmol) were added to the flask. TEA (41 μL, 0.294 mmol) was added, and the solution was stirred for 24 h. The solvent was then removed by evaporation under reduced pressure. The product was purified by dissolving the residue in a minimal amount of CH_2Cl_2 (500 μL) and then precipitating the salts by addition of Et_2O (5 mL). Filtration through celite removed the salts, and the solvent was removed by evaporation under reduced pressure to afford **6.26** as a yellow oil (17.4 mg, 0.108 mmol, 60% yield).

Diazomalonate 6.27. A round-bottomed flask (10 mL) was charged with CH_2Cl_2 (2 mL), EtOH (25 μL, 0.687 mmol), and 2-bromoethanol (30 μL, 0.421 mmol). This mixture was stirred rapidly while malonyldichloride (20 μL, 0.206 mmol) was added dropwise at room temperature. ESMS showed complete conversion to the 2-bromoethyl ethylmalonate within 2 h. The solvent and excess reagents were removed by evaporation under reduced pressure, and then MeCN (2 ml) and pyridine (50 μL) were added to the flask. After 24 h, *p*-acetamidobenzylsulfonyl azide (94.1 mg, 0.392 mmol) and then TEA (150 μL, 1.076 mmol) were added. The solution was then stirred for another 12 h. The solvent was then removed by evaporation under reduced pressure to afford **6.27**; the yield was qualitatively estimated to be ~50% by MS (*m/z* 264.3).

Diazomalonate 28. To a stirred, dry solution of penta(ethylene glycol) (44.4 μL, 0.210 mmol), CH_2Cl_2 (20 mL), and TEA (150 μL, 1.076 mmol) was added malonyl dichloride (24 μL, 0.247 mmol). The mixture was heated to reflux for 5.5 h, cooled, and then the solvent was removed by evaporation under reduced pressure. The product was recovered by extraction of the crude residue with refluxing hexanes (20 mL). The

benzene was then removed by evaporation under reduced pressure to leave the malonate crown ether. This malonate ester[15] was then dissolved in MeCN (3 mL). Stepwise addition of *p*-acetamidobenzenesulfonyl azide (151.0 mg, 0.629 mmol) and TEA (200 μL, 1.435 mmol) provided **6.28** after stirring for 10 h. The solvent was removed *in vacuo*, the residue was dissolved in a minimal amount of CH_2Cl_2 (500 μL), and the undesired salts precipitated out of solution with the addition of Et_2O (5 mL). Filtration through celite and removal of solvent by evaporation under reduced pressure yielded **6.28** (59.3 mg, 0.179 mmol, 85% yield).

Diazomalonate 6.29. To a stirred, dry solution of 18-crown-6-methanol (50.0 μL, 0.159 mmol), CH_2Cl_2 (1.5 mL), and TEA (33 μL, 0.237 mmol) was added ethyl malonyl chloride (28 μL, 0.219 mmol). The mixture was heated to reflux for 8 h, the solution was cooled, and then the solvent was removed by evaporation under reduced pressure. The residue was dissolved in MeCN (750 μL), and treated with TEA (30 μL, 0.215 mmol). To this solution was added *p*-acetamidobenzenesulfonyl azide (53.1 mg, 0.221 mmol), and the mixture was stirred for 10 h. The solvent was removed by evaporation under reduced pressure, the residue dissolved in a minimal amount of CH_2Cl_2 (500 μL), and the undesired salts were precipitated out of solution with the addition of Et_2O (5 mL). Filtration through celite and removal of solvent by evaporation under reduced pressure yielded **6.29** (59.8 mg, 0.138 mmol, 87% yield) as a light yellow oil. A small sample (~15 mg) was chromatographed to analytical purity by HPLC (0.1% (wt/v) TFA in water, 8.0 mL/min, 0.30% acetonitrile/min, 82-85 min). FTIR (thin film) 2879, 2142, 1755, 1689; ^{1}H NMR (300 MHz, $CDCl_3$) 4.45 (dd, J = 3.85, 12.1 Hz, 1H), 4.31 (q, J = 7.14 Hz,

2H), 4.27 (m, 1H), 3.85 (t, J = 4.95), 3.80 (br s, 1H), 3.67 (br s, 21H), 1.32 (t, J = 7.14 Hz, 3H); MS m/z 435.2 (H^+).

6.3 Results and Discussion.

Copper (I) and Silver (I). The ESI-MS spectrum for a mixture of copper (I) and **6.1** is shown in Figure 6.1a. The base peak corresponds to [**6.1**+MeCN+Cu]$^+$ or **6.3** (for simplicity, the corresponding structures are to the right of the mass spectra in Figure 6.1). It can also be seen from Figure 6.1a that **6.1** has a high affinity for Na^+ (present as an impurity) and that Cu (I) has a high affinity for acetonitrile. As seen in Figure 6.1b, isolation of **6.3** followed by CAD leads to sequential losses of 28 Da. The first loss of 28 Da corresponds to the loss of N_2 from the diazo functionality leading to structure **6.4**. Spontaneous Wolff rearrangement of **6.4** is accompanied by the second loss of 28 Da, which is attributed to be a loss of CO yielding **6.5**. In Figure 6.1c, structure **6.5** is isolated and subjected to further CAD resulting in another loss of 28 Da. This is also attributed to Wolff rearrangement of **6.5** followed by the loss of a second CO yielding the stable copper Fischer carbene **6.6**. Figure 6.1d shows the results of CAD of structure **6.6**. In this case, the noncovalent acetonitrile adduct is lost, followed by the pickup of either water or methanol. This pickup is not surprising given the vacant copper (I) coordination site and the fact that the spectra were acquired from a water/methanol solution.

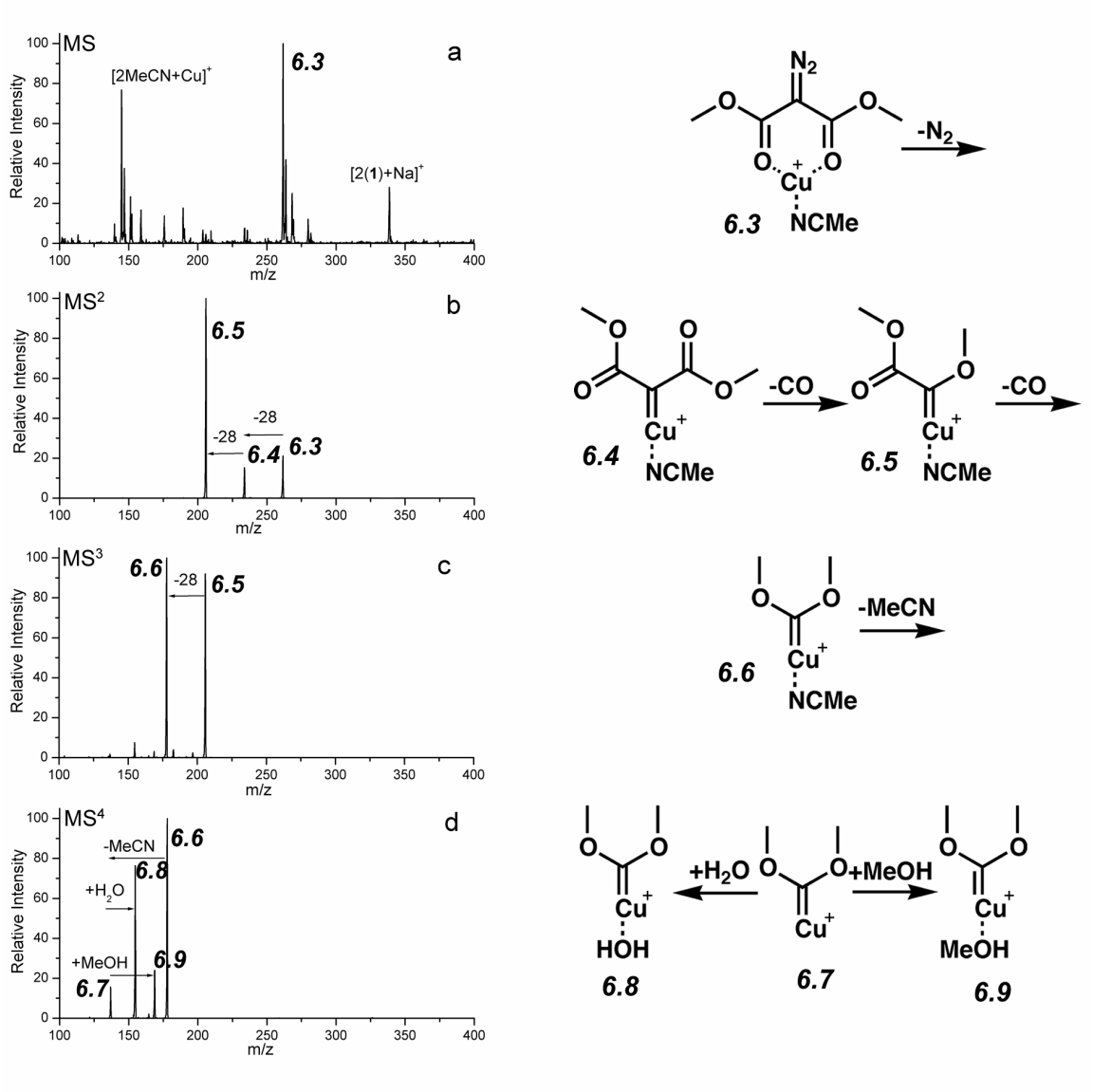

Figure 6.1 Structures for the peaks in the mass spectra on the left are provided in the reaction scheme to the right. (a) MS of a mixture of **6.1** and Cu (I) in a 20/80 (v/v) water/methanol solution with ~0.1% MeCN. (b) MS^2 on complex **6.3**. N_2 and CO are lost sequentially. (c) MS^3 on complex **6.5** resulting in the loss of an additional CO. (d) MS^4 on **6.6** resulting in the exchange of the MeCN ligand for either water or methanol.

DFT calculations at the B3LYP level using the LACVP** basis set were performed to determine structures and relative energetics for the products and probable intermediates in Figure 6.1. The structures and energetics are presented in the reaction coordinate diagram in Figure 6.2. When a ligand such as N_2 or CO is lost, the energy of the minimized separated molecule is added to compare with the complex prior to dissociation. Structure **6.3** is found to be the global minimum, and there is support for this binding mode from crystal structures.[16] Direct dissociation of N_2 from **6.3** is unlikely because the copper (I) ligand restrains the geometry of the molecule in a triplet-like conformation, whereas the thermal dissociation of N_2 must yield the singlet state.[17] Furthermore, **6.1** has a singlet ground state[5], and attempts to minimize structure **6.3** with the N_2 removed were unsuccessful. Matrix isolation studies on similar systems suggest that copper (I) insertion into the C-N bond of **6.3** is a more likely alternative.[18]

Further experimental and theoretical evidence also suggests that the copper (I) ion mediates the generation of the carbene from the diazo precursor. CAD experiments on [**6.1**+Na]$^+$ result in the complete loss of signal without producing any observable peaks, suggesting dissociation of the sodium ion (which has m/z ratio that is too small to detect). Similar experiments with rubidium yield a peak corresponding to Rb^+ exclusively from the collisional activation of [**6.1**+Rb]$^+$. The calculated ΔH for reaction 6.1 is -59 kcal/mol, which can be regarded as the binding energy of the sodium ion to **6.1**.

$$\mathbf{6.1} + Na^+ \rightarrow \mathbf{6.1}\cdot Na^+ \qquad (6.1)$$

$$\mathbf{6.1}\cdot Cu + MeCN \rightarrow \quad \mathbf{6.3} \qquad (6.2)$$

Similarly, calculations reveal a ΔH of -43 kcal/mol for reaction 6.2, which is the binding energy of MeCN to the **6.1**·Cu complex. This value is in reasonable agreement with similar experimental and theoretical results.[19] The MeCN ligand is retained

throughout the entire series of reactions shown in Figure 6.2 without dissociating. Therefore the reaction barriers for each step must be below 43 kcal/mol, otherwise the MeCN ligand would simply dissociate. Furthermore, the binding energy of the sodium ion is much greater at 59 kcal/mol, yet the ion dissociates prior to the loss of N_2 and the generation of the carbene. This demonstrates that copper (I) lowers the activation barrier for the generation of a carbene by at least 16 kcal/mol relative to complexation with sodium.

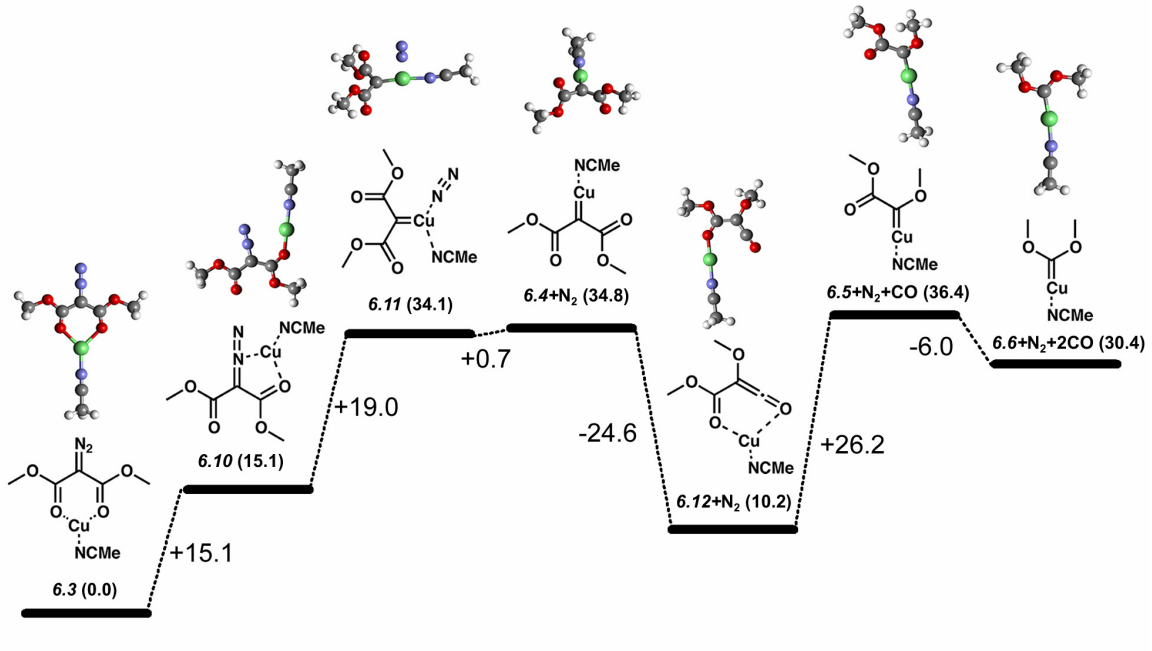

Figure 6.2 Reaction coordinate diagram including intermediate structures for the reactions in Figure 6.1. The energetics are calculated relative to structure **6.3** and are given in parentheses in kcal/mol. When a neutral gas molecule is lost the energy of the minimized, separated molecule is added to that of the remaining structure. See the text for a discussion of the barriers at each step.

The reaction shown in Figure 6.2 proceeds by rearrangement of structure **6.3** to structure **6.10** followed by Cu^+ insertion as shown in **6.11**. Crystal structures of copper (I) Fischer carbenes have similar C-Cu bond lengths to those in **6.11**, and in some cases demonstrate a high affinity for MeCN ligands.[20] Copper insertion is postulated as a prelude to the Wolff rearrangement from **6.4** to **6.12**, which must proceed through a singlet state. There is poor agreement between theoretically and experimentally determined barriers to Wolff rearrangement, with theory predicting higher values than those observed experimentally.[21] Theory would predict a large barrier for the conversion of **6.4** to **6.12** because of the exothermicity of the reaction.21[b] The experimental evidence in Figure 6.1b suggests that both rearrangement of **6.4** to **6.12** and subsequent loss of CO to produce **6.5** proceed with minimal barriers. It should be pointed out that, given a low barrier to rearrangement, the structure for the observed peak in Figure 6.1b may be the rearranged product (**6.12**) rather than carbene (**6.4**).[22] In either case, the observed products suggest that the presence of copper lowers the barrier to Wolff rearrangement in addition to facilitating the generation of the initial carbene.

The Wolff rearrangement product of **6.5** undergoes copper insertion without barrier upon minimization, suggesting that the transition state may occur prior to rearrangement. Therefore, the loss of the second CO likely occurs in a concerted fashion without a true ketene intermediate. The data in Figures 6.1b and 6.1c shows that the initial two losses occur simultaneously, which suggests a higher barrier to the loss of the second CO. However, it should be noted that the non-covalently bound MeCN ligand is retained throughout the entire process, limiting the reaction barriers to the bond dissociation energy of the Cu-NCMe bond (or 43 kcal/mol). Finally, a stable Fischer carbene (**6.6**) is produced upon loss of the second CO. Subsequent excitation of this complex results in

the loss of the MeCN ligand followed by attachment of either H_2O or MeOH from the residual solvent vapor present in the ion trap (Figure 6.1d).

In the presence of silver (I), structure **6.13** (Figure 6.3a) is formed in high abundance. However upon collisional activation in Figure 6.3b, the MeCN ligand is lost instead of N_2 as was the case with copper (I). This difference is due to the weak binding of the third ligand to the silver (I) cation.[23] Loss of the MeCN adduct is followed by collisional cooling of the product (**6.14),** which leads to some pickup of residual methanol (**6.15**) or water (**6.16**) from the trap as seen in Figure 6.3b. Further CAD of re-isolated **6.14** leads to the exclusive loss of 56 Da, comprising N_2 and CO with no intermediate loss of N_2 being observed. Again these losses are followed by the pickup of methanol or water. The absence of an intermediate loss of N_2 suggests that silver (I) is more efficient at facilitating the Wolff rearrangement and subsequent loss of CO than copper (I), consistent with the predominant use of silver (I) as the catalyst where Wolff rearrangement is required for a synthetic route.[4a] Isolation and activation of **6.17** leads to the expected loss of the second CO, yielding structure **6.20** and ensuing pickup of water or methanol. The silver Fischer carbenes **6.20**, **6.21**, and **6.22** are the final observable carbene products in this sequence. Further CAD of **6.20** leads to the loss of the Ag^+ cation, presumably generating the neutral dimethoxy carbene in the process.

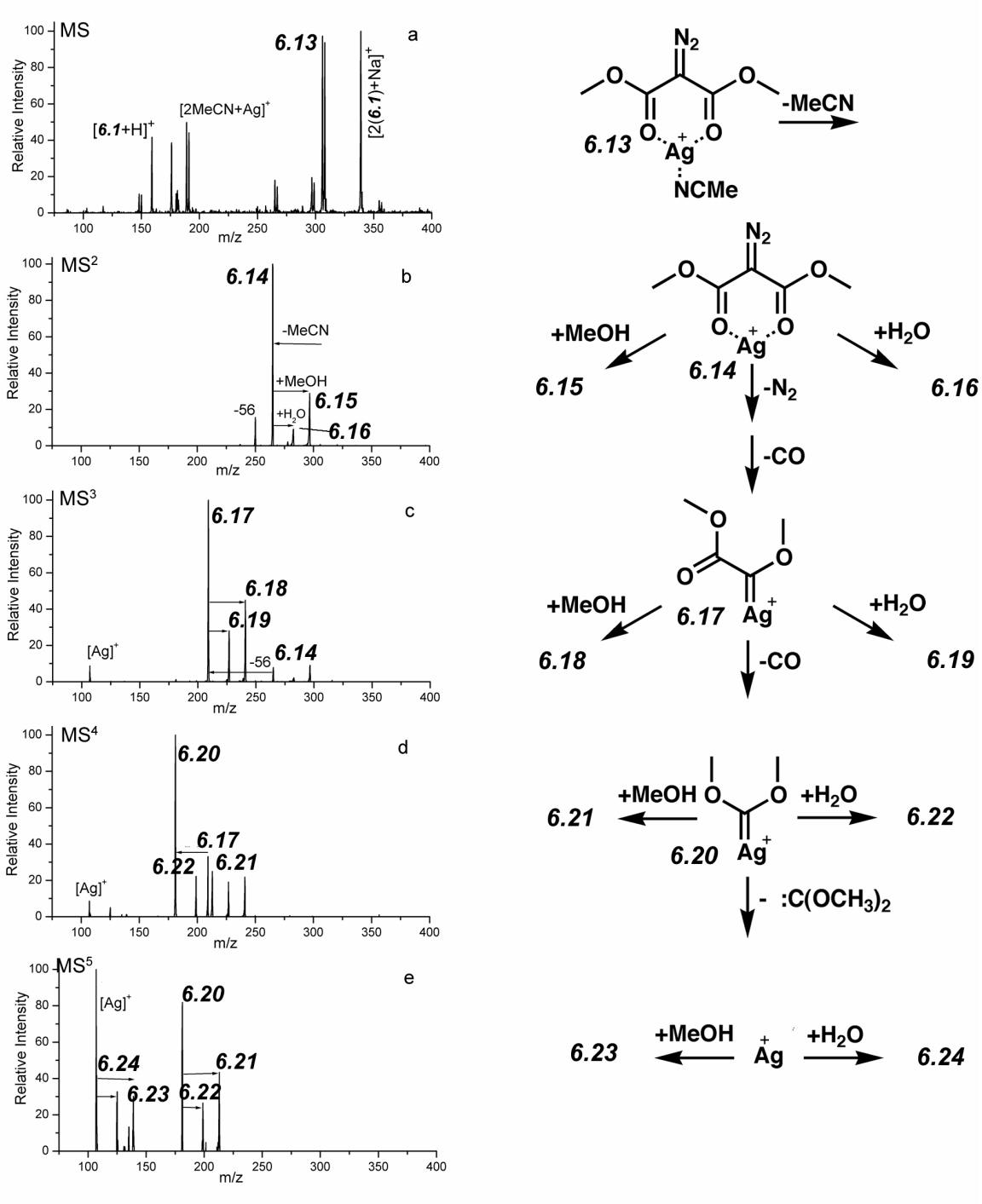

Figure 6.3 Spectra acquired from a mixture of silver (I) and **6.1**. The structures are given to the right of the appropriate spectrum. (a) MS spectrum showing complexation with Ag^+. (b) MS^2 spectrum of **6.13**, where the loss of MeCN generates the most abundant product ion peak. (c) MS^3 spectrum of **6.14** showing the facile loss of N_2 and

CO. (d) MS^4 spectrum of **6.17** showing loss of second CO and generation of final silver Fischer carbenes. (e) MS^5 spectrum of **6.20**, further CAD results in the cleavage of the metal/carbon bond.

Labeling Experiments. Isotopic labeling experiments were performed to confirm the proposed reaction pathways. The results for the two labeled compounds, **6.25** and **6.26**, are given in Table 6.1. Structure **6.25** is labeled with three deuteriums on each of the terminal methyl groups. Comparison of the data in Table 6.1 with that shown in Figure 6.1 reveals that the six deuteriums are retained throughout the entire experiment. This indicates that only interior carbons are lost as CO and that there is no detectable scrambling with MeOH in the ion trap. In order to confirm which carbons are lost and to determine the extent to which rearrangement of the carbene occurs, structure **6.26** was synthesized with ^{13}C at the 1,3 positions. Experiments with **6.26** confirm that the two interior ^{13}C labeled carbons are lost, as shown in Table 6.1. There is no apparent rearrangement of the carbene via an oxirene intermediate as depicted in Scheme 6.2.[10] These two experiments serve to confirm that N_2 is lost first, as is expected, and that carbon in the 1 and 3 positions specifically, are lost as CO.

Scheme 6.2 Potential carbene scrambling via oxirene (not observed).

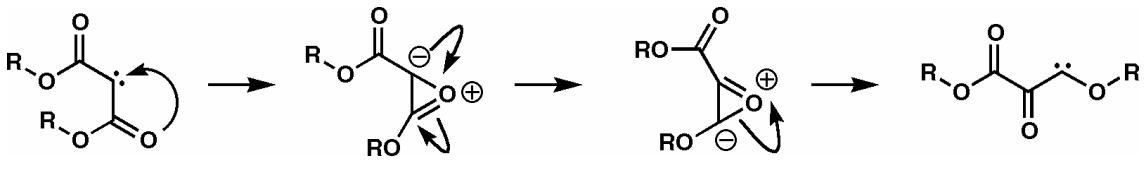

Divalent Metals, Protons, and Fixed Charges. The experimental MS data for several related experiments on **6.1** are summarized in Table 6.1. For both copper (II) and nickel (II), the metal is complexed with three molecules of **6.1** or $[3(\mathbf{6.1})+M]^{2+}$ (where M = Ni or Cu), with the ligands coordinating the metal in a pseudo-octahedral fashion. CAD of these complexes does not lead to the loss of N_2, but instead yields only the loss of an entire coordinating molecule. A small amount of $[\mathbf{6.1}+Cu+2MeCN]^{2+}$ is also formed from the copper solution. However, as the data shows in Table 6.1, this complex simply loses one of the MeCN ligands upon CAD. These results illustrate that copper (II) and nickel (II) are not efficient at mediating the formation of Fischer carbenes or subsequent Wolff rearrangements. Protonated **6.1** does not lose N_2 upon CAD either, but instead yields the assortment of fragments shown in Table 6.1.

The results presented thus far suggest that the coordinating charge can dictate the resulting chemistry upon collisional activation in diazo compounds. Structure **6.27** was designed to investigate the energetics of N_2 loss and Wolff rearrangements in the absence of a coordinating charge. In **6.27**, the charge is provided by a fixed quaternary nitrogen from the pyridinium group. As seen in Table 6.1, this compound loses N_2 to yield the most abundant product by CAD in the MS^2 spectrum. Further collisional activation of the resulting molecule demonstrates that Wolff rearrangement and the loss of multiple CO molecules does occur. However, this process is accompanied by other losses not related to Wolff rearrangement. In fact, the loss of pyridine yields the base peak in the MS^3 spectrum. This suggests that the energetics associated with Wolff rearrangement and loss of CO for this reaction are similar to those for the loss of pyridine. Quantitative CAD experiments on related quaternary pyridinium molecules suggest that the loss of pyridine is not likely to require more than ~60 kcal/mol activation energy but may require

substantially less.[24] This can be regarded as the upper limit for the activation barrier to Wolff rearrangement and dissociation of CO for these experiments.

Table 6.1. Summary of MS results.

Molecule	Cation	Initial Ligands	Observed Peaks†
6.25	Cu^{+}	MeCN	MS^2 on 268→ 193(12), 212(100), 240(15), 268(21) MS^3 on 212→ 161(11), 184(100), 212(80) MS^4 on 184→ 143(5), 161(43)*, 175(8)*, 184(100)
6.26	Cu^{+}	MeCN	MS^2 on 264→ 207(100), 236(11), 264(2) MS^3 on 207→ 178(100), 207(98)
6.1	Cu^{2+}	2(**1**)	MS^2 on 268.4→ 189.5(100), 268.4(<1)
6.1	Cu^{2+}	2MeCN	MS^2 on 151→ 140(100)*, 147(50)*
6.1	Ni^{2+}	2(**1**)	MS^2 on 266→ 187(30), 196(100)*, 203(72)*, 266(<1)
6.1	H^{+}	--	MS^2 on 159→ 55(80), 69(6), 87(100), 101(8), 127(93), 145(28), 159(<1)
6.2	Cu^{+}	MeCN	MS^2 on 414→ 345(8), 373(100), 414(10) MS^3 on 373→ 289(55), 317(37), 345(42), 373(100)
6.2	Ag^{+}	--	MS^2 on 417→ 289(12), 317(17), 333(39), 345(25), 361(96), 389(100), 417(16) MS^3 on 389→ 317(10), 333(26), 361(69), 389(100)
6.27	See structure	--	MS^2 on 264→ 113(8), 157(13), 236(100), 264(22) MS^3 on 236→ 157(100), 180(42), 192(40), 208(61), 236(57)

†Peaks are given with accompanying relative intensities in parentheses. Some low intensity peaks (under 15% relative intensity) that are not assigned structures or discussed in the text are omitted for clarity.

*Solvent molecule pickups

The pattern of losses for molecule **6.27** contrasts sharply with the results obtained for all of the copper (I) and silver (I) adducts. Metal adducts of **6.1** lose N_2 and the first CO in one step without the addition of further excitation energy. The loss of the second CO occurs upon further activation, but no other competitive products are produced in significant abundance at any stage of the experiment. In the case of **6.27**, N_2 loss occurs without any accompanying loss of CO. Upon further excitation of $[\mathbf{6.27}\text{-}N_2]^+$, Wolff rearrangement followed by the loss of the first and second CO molecules occurs spontaneously with the appearance of several other competitive products. In other words, Wolff rearrangement products are no longer favored in the absence of a metal ligand. These results suggest that copper (I) and silver (I) facilitate the Wolff rearrangement and loss of CO shown in Figures 6.1 and 6.2.

Chart 6.1

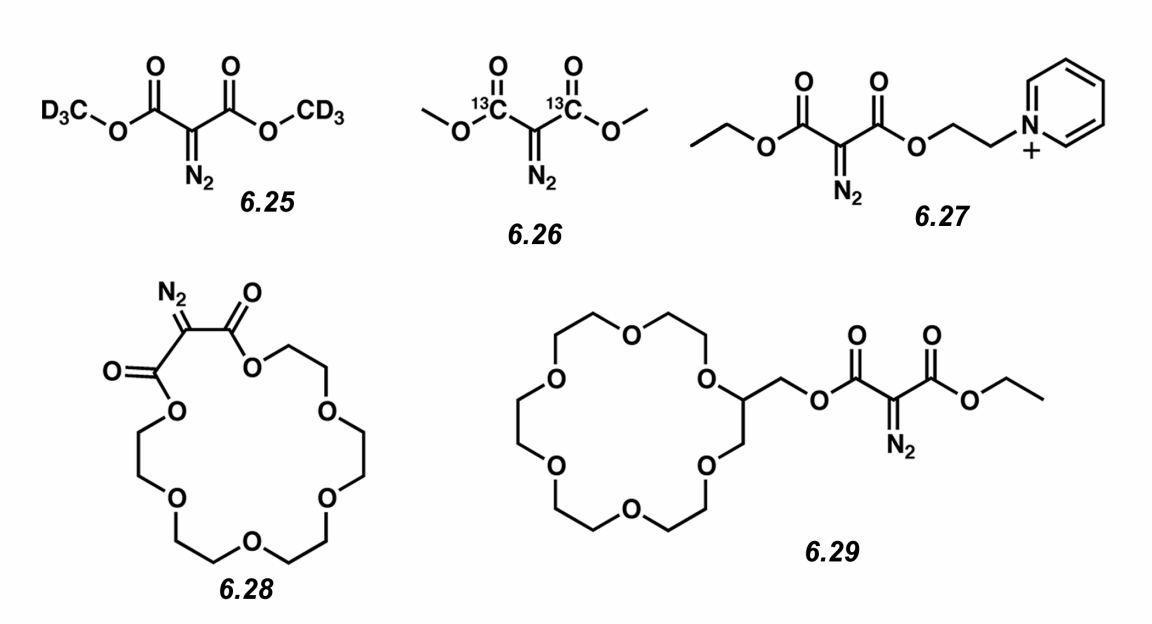

Effect of Benzyl Groups. In structure **6.2** the methyl groups are replaced by benzyl groups, and with the addition of copper (I) the ESI-MS contains a prominent [**6.2**+Cu+MeCN]$^+$ peak. As shown in Table 6.1, CAD dissociation of this peak leads primarily to the loss of the MeCN ligand. No appreciable pickup of water or methanol is observed following the loss of MeCN. This suggests that the benzyl groups are able to coordinate the metal ion sufficiently so that the lost ligand is not replaced. There is precedence for this type of coordination from crystal structure studies.[25] Interestingly, further CAD of [**6.2**+Cu]$^+$ leads to the sequential loss of N_2, CO, and CO with each intermediate being observed. No further activation is necessary to observe the loss of all three molecules. Similar experiments with silver (I) and **6.2** yield very similar results (Table 6.1), but in this case the [**6.2**+Ag]$^+$ peak is formed directly from solution in high abundance. Because the metal ion is coordinated to **6.2** by the benzyl groups, the relative conformation of the diazo functionality to the esters is different for copper (I) and silver (I) adducts of **6.1** and **6.2**. DFT calculations suggest a structure similar to the silver (I) adduct shown in **6.30**. The fact that Wolff rearrangement proceeds more easily for **6.30** than for **6.3** suggests that the conformational energy minimum is similar to the preferred conformational orientation that leads to Wolff rearrangement for **6.30**. Conformational effects have been observed to influence Wolff rearrangements previously.[10]

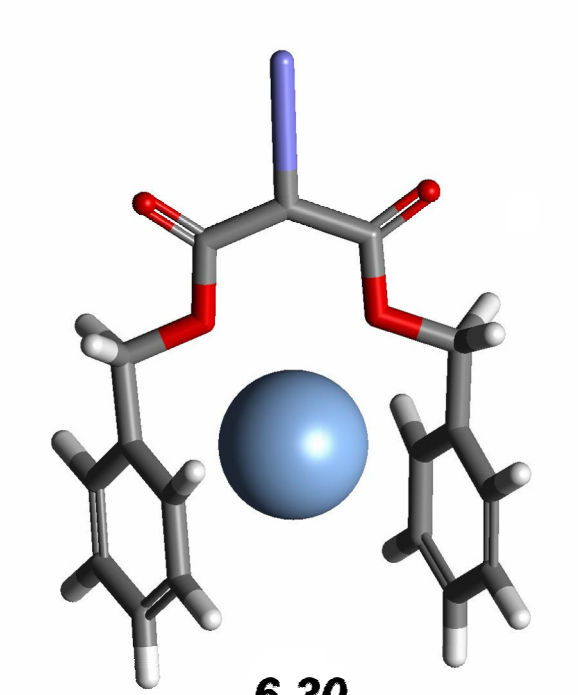

6.30

Macrocycles. Crown ethers and other related macrocycles are well suited to coordinate a variety of charge bearing groups[26] and usually exclude the presence of other solvent adducts once in the gas phase. Therefore, structures **6.28** and **6.29** are well suited to study the effects of various cations and different coordination motifs on the Wolff rearrangement in the absence of third party ligands. The diazo group for **6.28** is included in the ring, bringing the charge in close proximity to the diazo group. However, it should be noted that the coordination geometry between the charge and the diazo is significantly different for **6.1** and **6.28** due to the conformational restraints of the macrocyle. Structure **6.29** is more dynamic, allowing for either coordination or separation of the metal and the diazo group, depending primarily on the temperature of the molecule as explained below.

The CAD results for **6.28** coordinated to copper (I) and sodium are presented in Table 6.2. In both cases, the loss of N_2, CO, and CO occurs predominantly one step at a time, requiring the acquisition of an MS^4 scan to induce the loss of the second CO. This

suggests that the more conformationally restrained macrocycle requires additional activation energy to induce Wolff rearrangement, but does not necessarily exclude participation of the cation in the reaction. The resonance excitation RF voltages applied at each step of the experiment are (for sodium) 0.67V, 0.83V, 0.99V and (for copper) 0.69V, 0.82V, 0.71V respectively. The excitation voltages are very similar for the first two steps of the experiment for both cations, but copper (I) clearly catalyzes the loss of the second CO more efficiently than sodium ($\Delta V \sim 0.3V$). This is additionally confirmed by the absence of competitive fragments in the copper (I) experiment, whereas in the case of sodium the base peak in the MS^4 spectrum is not the product of Wolff rearrangement.

The copper (II) adduct of **6.28** can also be prepared in small abundance and the results for the CAD are found in Table 6.2. Copper (II) catalyzes the loss of 44, which is presumably the loss of ethylene oxide from the crown ether portion of the molecule.[27] The loss of N_2 is not detected, again suggesting that copper (II) does not catalyze the formation of Fischer carbenes or the subsequent Wolff rearrangement observed with other cations. CAD of the ammonium adduct of **6.28** is also presented in Table 6.2. In this case, the loss of NH_3 followed by subsequent cleavage of protonated **6.28** is the only process observed. This suggests that close proximity of a labile proton can prevent the loss of N_2 and subsequent reactions from occurring. However, it should be noted that this problem is easily corrected by complexation with a more basic amine such as 1-hexylamine. CAD of the hexylamine adduct leads primarily to the loss of N_2 (data not shown). Alternatively, weaker binding by ammonium versus 1-hexylamine may explain the dissociation in the case of ammonium. These experiments confirm the notion that the cation can greatly influence the subsequent chemistry upon excitation of these molecules.

Table 6.2 MS data for crown compounds

Molecule	Cation	Initial Ligand	Observed Peaks†
6.28	Na^+	--	MS^2 on 355→ 327(100), 355(6) MS^3 on 327→ 255(13), 271(6), 299(100), 327(5) MS^4 on 299→ 225(100), 255(40), 271(73), 299(18)
6.28	Cu^+	--	MS^2 on 395→ 339(26), 367(100), 395(18) MS^3 on 367→ 339(94), 367(100) MS^4 on 339→ 265(16), 311(100), 339(38)
6.28	NH_4^+	--	MS^2 on 350→ 173(11), 217(12), 261(100), 333(33), 350(72)
6.28	Cu^{2+}	--	MS^2 on 197.5→ 175.5(100), 184.3(6)*, 191.2(21)*, 197.5(5)
6.29	NH_4^+	--	MS^2 on 452→ 380(12), 424(100), 452(61) MS^3 on 424→ 175(26), 203(21), 247(19), 291(19), 351(44), 424(100)
6.29	Na^+	--	MS^2 on 457→ 385(3), 429(100), 457(9) MS^3 on 429→ 299(10), 357(29), 373(100), 385(10), 401(20), 429(30)

†Peaks are given with accompanying relative intensities in parentheses. Some low intensity peaks (under 15% relative intensity) that are not assigned structures or discussed in the text are omitted for clarity.

*Solvent molecule pickups

Charge proximity effects. In the copper (I) and silver (I) adducts of **6.2**, the metal ion is coordinated to the benzyl groups and is not in close proximity to the diazo group. It is not surprising that the resulting CAD spectra are very similar for both metals. In general, charges that are not in close proximity to the diazo group have less influence on the resulting CAD patterns. This is well illustrated by comparing **6.28** and **6.29**. Molecular dynamic simulations suggest that the collisional heating of **6.29** leads to extended structures where the lariat side arm extends away from the charge. This leads to a large separation between the charge and the diazo group. For structure **6.28**, heating of the quasimolecular complex does not lead to significant structural changes, leaving the charge in close proximity to the diazo group. The net effect is that the diazo group is ~2Å further away from the charge in **6.29** when compared to **6.28**. CAD of [**6.28**+NH_4]$^+$ does not lead to the loss of N_2 or subsequent Wolff rearrangement products. By contrast when **6.29** is complexed with ammonium, CAD leads to the loss of N_2 and formation of a carbene (Table 6.2). This implies that the ammonium ion does not interact with the diazo group in **6.29**, but this does not rule out subsequent interactions between the newly generated carbene and the cation. Interestingly, subsequent CAD of [**6.29**-N_2+NH_4]$^+$ does not lead to any Wolff rearrangement products. This is attributed to the high proton affinity of the carbene,[28] which reacts with the ammonium and prevents Wolff rearrangement. CAD of **6.29** complexed with sodium leads to the expected loss of N_2 and the formation of both Wolff rearrangement products in the MS^3 spectrum. Alternatively, weaker binding of ammonium by **6.28** relative to **6.29** may explain the difference in experimental results.

Conformational effects. The degree of conformational restraint present in a molecule can favor or disfavor subsequent Wolff rearrangement. It was established in the previous

paragraph that copper (I) and silver (I) adducts of **6.2** behave very similarly with the simultaneous loss of all products, but it should be noted that the CAD spectra of these two complexes are not similar to any others obtained in the course of this study. We attribute this to a conformational effect where the metal restrains the molecule in a conformation that favors Wolff rearrangement. The opposite effect is observed in [**6.28**+Na]$^+$, which is also conformationally restrained. In this case Wolff rearrangement is not favored, and additional activation energy must be added at each step. Interestingly, the barrier becomes much larger when the diameter of the macrocycle is reduced. This supports the proposition that conformational constraints lead to the larger activation barriers required for the CAD of **6.28** bound to various ions. Unconstrained systems with a remote charge that does not react with the carbene such as **6.27** and [**6.29**+Na]$^+$ all demonstrate similar behavior upon CAD.

Intermolecular reactions. Given the spectator MeCN ligand present in **6.3**, the possibility for intermolecular reactions might exist given the addition of the proper ligand. The results for attaching three different ligands are summarized in Table 6.3. It is easily seen in Table 6.3 that in each of these experiments the ligand is lost (either competitively or exclusively) at some point in the experiment. This suggests that the binding energy of the ligand to the copper (I) cation is not greatly increased by the presence of the additional functional groups. In particular, 5-hexynenitrile is not strongly bound to copper (I). Therefore, if the loss of the weakly bound noncovalent ligand is not observed, but a covalent bond cleavage occurs which interrupts the established sequential rearrangement processes (i.e., loss of N_2, CO, CO), then it is assumed that an intermolecular reaction has occurred. The reactions that lead to subsequent cleavages are complicated and it is not our intention to fully describe them here. However, it is shown

from the results that alkynes are much more reactive than analogous alkenes. This is not an unusual result given the greater reactivity of alkynes in general. Similarly, the observed reactivity of the phenyl group was unexpected. In the case of **6.2**, the benzyl groups ultimately displaced the ligand and prevented any reactions from occurring.

It is also interesting to note that CAD of [**6.1**+hexynenitrile+Cu]$^+$ yielded the loss of a neutral methyl radical in the MS^3 spectrum. This unusual loss was confirmed by experiments with **6.26** in which the loss of CD_3 was observed. The loss of methyl radical is accompanied by the pickup of water or methanol. It is unlikely that the methyl group was a metal ligand prior to dissociation, so an alternative explanation is required to explain the pickup of water and methanol. One possible explanation for this involves the oxidation of the copper (I) to copper (II) accompanied by the reduction of the newly formed terminal CO_2. The oxidation to copper (II) would create a new vacant ligand site and lead to the observed pickups. The exact role of the alkyne in this process remains unclear, but it may serve to stabilize the higher oxidation state of the copper.

Table 6.3 Intermolecular reactions with Fischer carbenes.

Molecule	Cation	Initial Ligand	Partial Loss of Ligand	Covalent Bond Cleavage†
6.1	Cu^+	5-hexynenitrile	yes	MS^3
6.2	Cu^+	5-hexynenitrile	yes	no
6.1	Cu^+	5-hexenenitrile	yes	no
6.1	Cu^+	4-phenylbutyronitrile	yes	MS^3

†If covalent bond cleavage occurs either competitively with loss of the ligand or exclusively, the step where this occurs is indicated.

6.4 Conclusions

In summary, the synthesis of copper (I) and silver (I) Fischer carbenes from various diazo malonates in the gas phase is demonstrated for the first time. The carbenes are generated by the facile loss of N_2. The carbenes prepared by this process can undergo multiple Wolff rearrangements in the gas phase, which subsequently lead to the loss of multiple carbon monoxides. Surprisingly, up to six different carbenes or metallo-carbenoids can be produced in a single experiment. A series of control experiments that elucidate the effects of conformation and metal mediation on Wolff rearrangements are detailed. Although the data has been gathered from gas phase experiments, the results reveal general trends that should be applicable for either enhancing or deterring Wolff rearrangements in solution. Coordinated metal ions profoundly mediate the energetics of these reactions. Silver (I) is most efficient at initiating Wolff rearrangements followed by copper (I), but no mediation is required and molecules labeled with non-participating charges undergo similar chemistry at higher energies. Conformational effects are also found to be important in determining the requisite energy for Wolff rearrangement. Divalent metal ions and protons interfere with the loss of N_2 and do not promote the formation of carbenes.

6.5 References

[1] (a) Stevens, A. E.; Beauchamp, J. L. *J. Am. Chem. Soc*. **1978**, *100*, 2584-2585. (b) Stevens, A. E.; Beauchamp, J. L. *J. Am. Chem. Soc*. **1979**, *101*, 6449-6450. (c) Halle, L. F.; Armentrout, P. B.; Beauchamp, J. L. *J. Am. Chem. Soc*. **1981**, *103*, 962-963.

[2] Adlhart, C.; Hinderling, C.; Baumann, H.; Chen, P. *J. Am. Chem. Soc*. **2000**, *122*, 8204-8214.

[3] Bertani, R.; Michelin, R. A.; Mozzon, M.; Traldi, P.; Seraglia, R.; Busetto, L.; Cassani, M. C.; Tagleatesta, P.; D'Arcangelo, G. *Organometallics* **1997**, *16*, 3229-3233.

[4] (a) Doyle, M. P.; McKervey, M. A.; Ye, T. *Modern Catalytic Methods for Organic Synthesis with Diazo Compounds*; Wiley-Interscience: New York, 1998. (b) Moody, C. J.; Whitham, G. H. *Reactive Intermediates*; Oxford University Press: New York, 1992; 26-50. (c) Straub, B. F.; Hofmann, P. *Angew. Chem. Int. Ed*. **2001**, *40*, 1288-1290.

[5] Julian, R. R.; May, J. A.; Stoltz, B. M.; Beauchamp, J. L. *Angew. Chem. Int. Ed.* **2003**, *42(9)*, 1012-1015.

[6] (a) Marzluff, E. M.; Beauchamp, J. L. In *Large Ions: Their Vaporization, Detection, and Structural Analysis*; Baer, T., Ng, C. Y., Powis, I.; Eds.; John Wiley & Sons Ltd.: New York, 1996; 115-143. (b) McLuckey, S. A. *J. Am. Soc. Mass Spectrom*. **1992**, *3*, 599-614. (c) Hayes, R. N.; Gross, M. L. *Methods Enzymol*. **1990**, *193*, 237-263.

[7] Richardson, D. C.; Hendrick, M. E.; Jones, M. *J. Am. Chem. Soc*. **1971**, *93*, 3790-3791.

[8] Marfisi, C.; Verlaque, P.; Davidovics, G.; Pourcin, J.; Pizzala, L.; Aycard, J.-P.; Bodot, H. *J. Org Chem*. **1983**, *48*, 533-537.

[9] Wolff, L. *Justus Liebigs Ann. Chem*. **1902**, 325, 129.

[10] (a) Sudrik, S. G.; Chavan, S. P.; Chandrakumar, K. R. S.; Pal, S.; Date, S. K.; Chavan, S. P.; Sonawane, H. R. *J. Org. Chem*. **2002**, *67(5)*, 1574-1579 and references therein. (b) McMahon, R. J.; Chapman, O. L.; Hayes, R. A.; Hess, T. C.; Krimmer, H. P. *J. Am. Chem. Soc*. **1985**, *107*, 7597-7606. (c) Fenwick, J.; Frater, G.; Ogi, K.; Strausz, O. P. McMahon, R. J.; Chapman, O. L.; Hayes, R. A.; Hess, T. C.; Krimmer, H. P. *J. Am. Chem. Soc*. **1973**, *95*, 124-132. (d) Pomerantz, M.; Levanon, M. *Tetrahedron Lett*. **1991**, *32*, 995-998. Also see ref. 4a Chapter 9.

[11] Arduengo, A. J.; Dias, H. V. R.; Calabrese, J. C.; Davidson, F. *Organometallics* **1993**, *12*, 3405.

[12] Julian, R.R.; Beauchamp, J. L. *Int. J. Mass. Spectrom*. **2001**, *210*, 613-623.

[13] Falorni, M.; Dettori, G.; Giacomelli, G. *Tetrahedron: Asymmetry* **1998**, *9*, 1419

[14] Kametani, T.; Yukawa, H.; Honda, T. *J. Chem Soc. Perkin Trans. 1* **1990**, *3*, 571-577.

[15] Lamb, J. D.; Izatt, R. M.; Swain, C. S.; Bradshaw, J. S.; Christensen, J. J. *J. Am. Chem. Soc.* **1980**, *102*, 479-482.

[16] Dias, H. V. R.; Polach, S. A. *Inorg. Chem*. **2000**, *39*, 4676-4677.

[17] Wentrup, C. *Reactive Molecules: The Neutral Reactive Intermediates in Organic Chemistry*; John Wiley & Sons: New York, 1984; 177-264.

[18] Chang, S.-C.; Kafafi, Z. H.; Hauge, R. H.; Billups, W. E.; Margrave, J. L. *J. Am. Chem. Soc.* **1987**, *109*, 4508-4513.

[19] (a) Vitale, G.; Valina, A. B.; Huang, H.; Amunugama, R.; Rodgers, M. T. *J. Phys. Chem. A* **2001**, *105*, 11351-11364. (b) Chu, Y.; Yang, Z.; Rodgers, M. T. *J. Am. Mass Spectrom*. **2002**, *13*, 453-468.

[20] (a) Barluenga, J.; Lopez, L. A.; Lober, O.; Tomas, M.; Garcia-Granda, S.; Alvarez-Rua, C.; Borge, J. *Angew. Chem. Int. Ed*. **2001**, *40*, 3392-3394. (b) Tulloch, A. A. D.; Danopoulos, A. A.; Kleinhenz, S.; Light, M. E.; Hursthouse, M. B.; Eastham, G. *Organometallics* **2001**, *20*, 2027-2031.

[21] (a) Likhotvorik, I.; Zhendong, Z.; Tae, E. L.; Tippmann, E.; Hill, B. T.; Platz, M. S. *J. Am. Chem. Soc*. **2001**, *123*, 6061-6068. (b) Scott, A. P.; Platz, M. S.; Radom, L. *J. Am. Chem. Soc*. **2001**, *123*, 6069-6076.

[22] Similarly, it is impossible to distinguish experimentally whether structures **5** and **17** have already undergone Wolff rearrangement prior to experimental observation.

[23] Shoeib, T.; Aribi, H. E.; Siu, K. W. M.; Hopkinson, A. C. *J. Phys. Chem. A* **2001**, *105*, 710-719.

[24] Katritsky, A.R.; Watson, C. H.; Dega-Szafran, Z.; Eyler, J. R. *J. Am. Chem. Soc*. **1990**, *112*, 2471-2478.

[25] (a) Dattelbaum, A. M.; Martin, J. D. *Inorg. Chem*. **1999**, *38*, 6200-6205. (b) Wen, M.; Munakata, M.; Suenaga, Y.; Kuroda-Sowa, T.; Maekawa, M. *Inorg. Chim. Acta* **2002**, *332*, 18-24.

[26] Bradshaw, J. S.; Izatt, R. M.; Borkunov, A. V.; Zhu, C. Y.; Hathaway, J. K. *Comprehensive Supramolecular Chemistry*, Vol. 1; G. W. Gokel, Pergamon/Elsevier: Oxford, 1996; 35-95.

[27] Maleknia, S.; Brodbelt, J. *J. Am. Chem. Soc.* **1993,** *115*, 2837-2843.

[28] (a) Vogt, J.; Beauchamp, J. L. *J. Am. Chem. Soc.* **1975,** *97*, 6682-6685. (b) Pliego J. R.; DeAlmeida, W. B. *J. Chem. Soc. Faraday Trans.* **1997**, *93*, 1881-1883.